ORIGINAL PAPER

Mesh-capped probe design for direct pH measurements at an actively corroding metal surface

Jiabin Han · Bruce N. Brown · David Young · Srdjan Nešić

Abstract Quantitative characterization of surface reaction species improves understanding of reaction mechanisms, especially for heterogeneous reactions such as in corrosion and electrolysis. A universal mesh-capped surface pH probe was developed in order to investigate surface proton concentrations for aqueous metal dissolution/deposition reactions. This technique can be generally applied to characterize the surface pH either for bare metal reactions or metals corroding beneath a corrosion product film. Measurements with the new probe design have shown a good degree of reproducibility. The surface pH measurements during corrosion of mild steel have shown that a higher surface pH is achieved at the steel surface as compared with that of the bulk solution, just as predicted from theory. Chemical buffering effects on surface pH were observed during corrosion by contrasting the measurements obtained in HCl deaerated solutions with those containing CO_2, i.e., carbonic acid (H_2CO_3) and acetic acid (CH_3COOH/HAc) solutions. It was found that the surface pH was mainly controlled by the water chemistry and chemical buffer capacity. The surface pH is affected by the deposited corrosion scale porosity. A higher deviation of surface pH compared to the bulk value was observed for more dense layers with lower porosity.

Keywords Surface pH probe · Steel mesh · Corrosion · Electrochemistry · Carbon dioxide · Organic acids

1 Introduction

Local surface chemistry conditions can be very different than those in the bulk and become important when chemical reactions occur at an interface. For example, metal reactions under aqueous conditions usually involve electrochemical surface processes; amongst a variety of processes, these result in metal dissolution (corrosion) and deposition [1, 2]. Surface pH is recognized as a key local parameter that influences electrochemical reaction mechanisms and rates [3, 4]. Mathematical modeling, based on thermodynamic, kinetic and transport theories, has helped in the quantification of surface pH conditions [5–8]. However, not much has been achieved in terms of direct surface pH measurement at a corroding surface due to difficulties with probe design, manufacturing and operation. The objective of this project was to design and employ a simple and flexible surface pH probe for direct measurement of surface pH at a corroding surface.

The existing designs outlined in the open literature typically deployed direct or indirect measurement methods, as summarized in Table 1, and are briefly reviewed in the following sections.

J. Han · B. N. Brown · D. Young · S. Nešić (✉)
Institute for Corrosion and Multiphase Technology, Ohio University, 342 West State Street, Athens, OH 45701, USA
e-mail: nesic@ohio.edu

B. N. Brown
e-mail: bbrown@bobcat.ent.ohiou.edu

D. Young
e-mail: youngd1@ohio.edu

Present Address:
J. Han
Earth and Environmental Sciences Division (EES), Los Alamos National Laboratory, Los Alamos, NM 87545, USA
e-mail: jhan@lanl.gov

Table 1 Surface pH measurement methods

Methods	Application
Indirect	
Chemical indicator (e.g., photocurrent-pH plot) [9, 10]	Electrolysis
Rotating ring disc electrode [11]	Electrolysis
Direct	
Standard pH probe [12]	Corrosion
Microelectrode [13–19]	Corrosion, electrolysis
Mesh-capped flat pH probe [20–27]	Electrolysis

1.1 Indirect surface pH measurement probe design

Surface pH probe designs have been previously reported for indirect pH measurements during electrolysis processes. One is a pH-mapping technique [9, 10] where a semiconductor contacts the solution and responds to the pH due to depletion of its insulating layer. The resulting capacitance change can be recorded with a generated photocurrent. This design is relatively complex and involves elements which are not easy or cheap to obtain or manufacture. Another indirect method is surface pH measurement using a rotating ring electrode [11]. This technique is based on the pH-potential relation as defined by the Nernst equation and does not lend itself easily to extension to different corroding systems.

1.2 Direct surface pH measurement probe design

In some early research, standard pH probes were modified for direct surface pH measurement. Dražić [12], for example, coated a standard pH probe with a porous silver film used as a substrate for electrochemical deposition of iron. This probe was then applied to surface pH measurement during iron surface dissolution (corrosion). Disadvantages for this design (which was initially attempted in the present study) include its fragility as well as a host of issues related to the intricacies of its fabrication and operation.

A very commonly used direct surface pH measurement device is a pH microelectrode specially designed for surface pH measurement [13–19]. Microtips, typically ranging from 1 to 20 μm in diameter [14], have been fabricated as the sensing elements of microelectrode pH probes; these have been applied in corrosion surface pH measurement [13, 16] as well as diffusion layer pH profiling [14, 15, 17, 18]. A major shortcoming of this design is that it interferes with the mass transfer boundary layers near the solid surface.
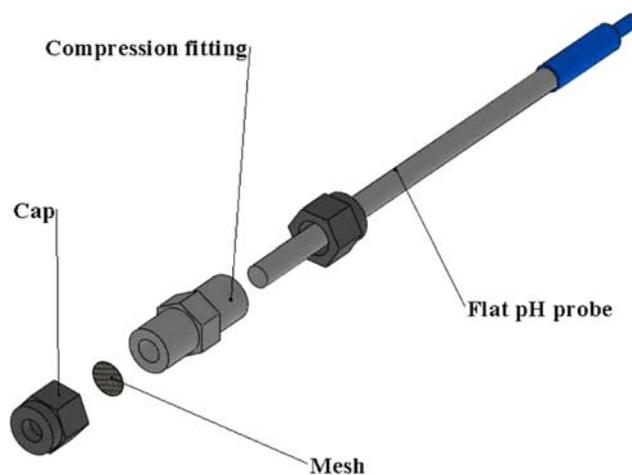
Another direct surface pH probe design was reported for electrolysis systems by Romankiw [20, 21]. The prototype

design consists of a flat sensor pH probe with a tip which is adhered to a metal mesh. During the corrosion of the mesh, surface pH can be monitored. This surface pH probe design was further modified for rotating [22] or fixed [23, 24] metal meshes. Particular applications were reported for surface pH measurement during jet impingement tests [24], electrodeposition [25, 26] and electrochemical reduction reactions [27]. This surface pH probe design concept was adopted as a starting point for the present design.

2 Experimental

2.1 Experimental design and setup

A simple probe design for surface and interfacial pH measurement was developed as shown in Fig. 1. The pH sensor used is a commercial flat pH glass probe. A compression fitting is employed to hold the pH probe body in place. A circular mild steel mesh is cut to match the size of the hollow compression fitting cap. This cap is used to push the mesh into tight adherence with the probe tip. This surface pH probe unit is inserted into the solution and the surface pH can be measured during the corrosion of the mild steel mesh. If needed, particulate materials used to simulate corrosion deposit layers can be filled in the cap and held trapped in place by another non-corroding mesh material (e.g., the stainless steel in the current study). The advantage of this design is its simplicity, portability, low fabrication cost and flexibility. The mesh can be easily mounted, removed and replaced. It can be easily deployed to determine surface pH measurement under electrochemical control by electronically connecting the mesh to a measurement instrument. The mesh can be easily obtained or manufactured out of most metals of interest, active, passive or noble, for corrosion studies, electrolysis,

Fig. 1 Surface pH probe design

catalysis, etc. Consequently, any set of heterogeneous reactions can be characterized in terms of metal surface pH.

In this study, the circular 3600 holes/in.[2] mild steel mesh was cut from a larger commercially available stock, to completely cover the pH probe surface. Details about the mild steel mesh used in the tests are listed in Table 2. The SEM images of an original single sheet mesh and a "double sheet compressed" mesh are depicted in Fig. 2. The compressed mesh was produced in order to reduce the mesh pore size and investigate if this has an effect on the performance of the probe.

The particles used to simulate the deposit layer were inert sand and glass beads, as shown in Fig. 3. The particle size for the sand ranged from 100 to 500 μm giving a bulk

Table 2 Mild steel mesh data

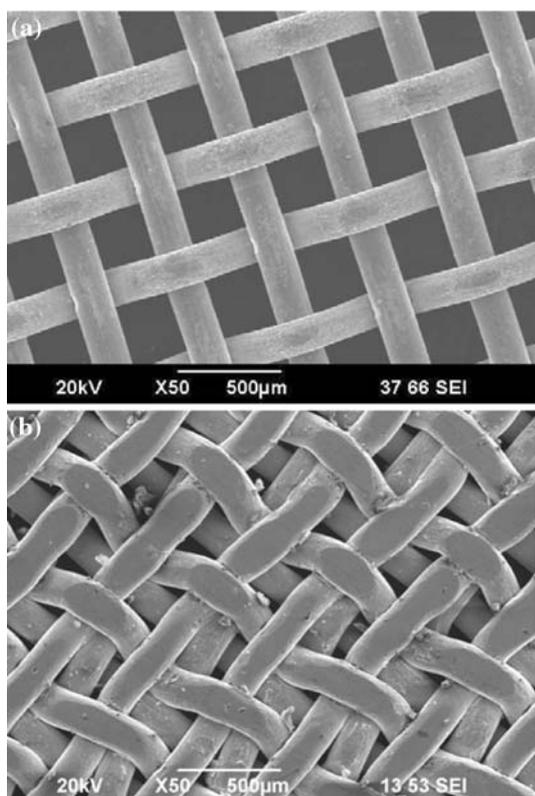| Steel type	Mild steel
Form	Woven wire cloth
Mesh size	60×60 holes/in.[2]
Square size	0.009 in.
Wire diameter	0.0075 in.
Mesh open area	30.5%

Fig. 2 SEM images of **a** single sheet mesh and **b** double sheet compressed mesh
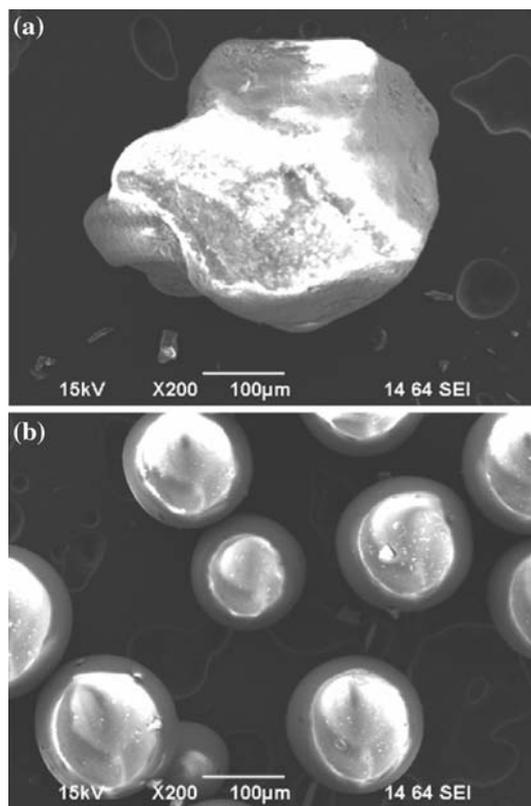

Fig. 3 The images of particles used to create the deposit **a** typical sand particle (size 100–500 μm) and **b** glass bead particles (size 50–80 μm)

layer porosity of approximately 40%. The smaller sand particles were 50–80 μm in size giving a bulk layer porosity of about 30%. Both were deposited in the form of a layer of 5 mm in thickness.

The meshed pH electrode was deployed in a standard three-electrode corrosion glass cell, as depicted in Fig. 4, filled with an aqueous solution. In this case, the measurements were performed under quiescent conditions. In different arrangements, flow can be readily created by other means (e.g., by flush mounting the probe at a pipe wall or a flow channel wall, using a jet impingement setup, etc.). All these alternatives appear to be easier than rotating the metal mesh, as was done by Romankiw [22].

2.2 Experimental test matrix and procedure

The test matrix for surface pH measurements is listed in Table 3. The effects of bulk pH, buffer capacity, temperature and surface layer porosity (achieved by using different particle sizes) were investigated.

A 1 wt% NaCl electrolyte solution was first deaerated by purging with CO_2 or N_2 in different experiments. Solution pH was adjusted with deaerated 1 M $NaHCO_3$ or 0.1 M HCl solutions as well as acetic acid when appropriate.

Table 3 Test matrix for the surface pH experiments

Mesh material	C1018 mild steel
Deposit material	Sand (porosity 40%), glass bead (30% porosity)
Depth of the deposit layer (mm)	5
Solution	CO_2–H_2O, HCl–H_2O, HAc–H_2O
Purge gas	N_2, CO_2
Temperature (°C)	25, 80
Gas partial pressure (bar)	0.97, 0.53
Bulk pH	4.0, 5.0, 6.0, 6.6
NaCl concentration (wt%)	1
Test period (h)	10

Temperature was controlled at 25 and 80 °C. The corresponding partial pressures of CO_2 are 0.97 and 0.53 bar given that the cell operated at atmospheric pressure.

Two pH probes, including a standard pH probe and a flat pH probe (fabricated for surface pH measurement), were first calibrated with standard buffer solutions at 4.00 ± 0.01, 7.00 ± 0.01 and 10.00 ± 0.01 pH units. The standard pH probe was then used to measure the bulk pH of the solution and the flat pH probe with the mild steel mesh was used for surface pH measurement. The steel mesh was first cleaned by immersing it in deaerated 0.1 to 0.5 M HCl solutions for about 10 min, or until oxidation products were removed and a shining metal mesh surface was produced. The mesh was then washed in isopropanol to dehydrate it and blown dry. It was mounted on the flat pH probe and tightened to the pH tip with the compression fitting cap holder. To measure the surface pH under a deposit layer, the small particles were filled as described in the design

section above. Both pH probes were immersed in the corrosive solution. The steel mesh corroded and the surface pH could be monitored and compared with the bulk solution pH.

3 Results and discussion

The meshed surface pH probe was used to measure the surface pH for mild steel corroding in different water chemistry conditions:
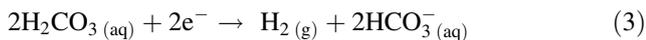
CO_2 saturated solution;
N_2 saturated HCl solution; and
N_2 saturated HAc solution.

From theory, the corrosion reactions for these environments can be summarized as two series of half-cell reactions: cathodic and anodic. The cathodic reactions in strong acid electrolytes, e.g., HCl solutions, are [28]:

$$2H^+_{(aq)} + 2e^- \rightarrow H_{2\,(g)} \tag{1}$$

$$2H_2O_{(l)} +\ 2e^- \rightarrow H_{2\,(g)} + 2OH^-_{(aq)} \tag{2}$$

The transport of reacting species from the bulk is often a limiting factor in these situations. For example, protons are consumed on the steel surface by a fast electrochemical reaction (1) and a decreased proton concentration, i.e., a higher pH, is expected on the surface compared to the bulk value.
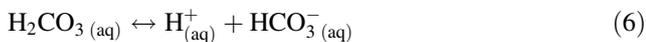
If weak acids, i.e., carbonic acid (H_2CO_3 obtained by hydration of dissolved CO_2) or acetic acid (HAc, CH_3COOH) are present, additional cathodic reactions need to be considered, such as [28, 29]:

$$2H_2CO_{3\,(aq)} + 2e^- \rightarrow H_{2\,(g)} + 2HCO_{3\,(aq)}^- \qquad (3)$$

$$2HAc_{(aq)} + 2e^- \rightarrow H_{2\,(g)} + 2Ac_{(aq)}^- \qquad (4)$$

The dominant anodic reaction is the oxidative dissolution of iron [28]:

$$Fe_{(s)} \rightarrow Fe_{(aq)}^{2+} + 2e^- \qquad (5)$$

It should be remembered that the two weak acids will partially dissociate to produce more protons and decrease the pH:

$$H_2CO_{3\,(aq)} \leftrightarrow H_{(aq)}^+ + HCO_{3\,(aq)}^- \qquad (6)$$

$$HAc_{(aq)} \leftrightarrow H_{(aq)}^+ + Ac_{(aq)}^- \qquad (7)$$

3.1 Validity and reproducibility of measurement using the surface pH probe

An initial series of experiments was conducted to confirm proper performance of the new pH probe. Figure 5 shows two sets of experiments conducted at 25 °C at bulk pH 4.0, in a CO_2 saturated electrolyte using a mild steel corroding mesh. After initial variation, a stable surface pH was measured which is approximately 1.5 pH units higher than the bulk pH. This translates into a surface proton concentration 50 times less than the bulk concentration, as calculated. Similar observations are shown in Fig. 6 for the bulk pH 6.0, even if the pH increase was not as large. Good reproducibility is obtained, which is within 0.1 pH units. This is considered to be in the error range of the pH probe measurement system.

The surface pH was measured using a single mesh and a compressed double mesh with a smaller pore size, as depicted in Fig. 2a and b, respectively. The surface pH, as shown in Fig. 7, is initially higher on the compressed mesh compared to that on the single mesh. In addition, steady state for surface pH measurement was achieved more rapidly for the compressed mesh. After an extended period of time, both probes reach approximately the same value.
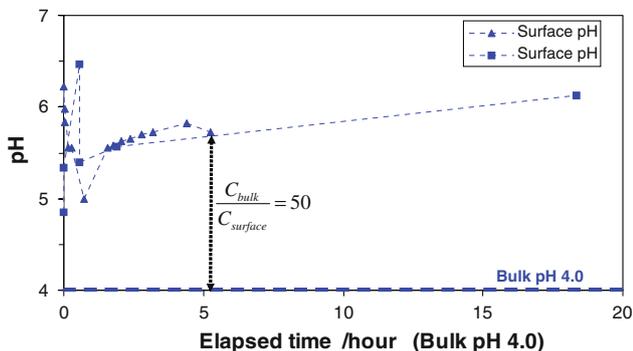

Fig. 5 Two series of surface pH measurements during mild steel mesh corrosion in a CO_2 purged solution at bulk pH 4.0, $T = 25$ °C, $p_{total} = 1$ bar, $p_{CO_2} = 0.97$ bar, $[NaCl] = 1$ wt%
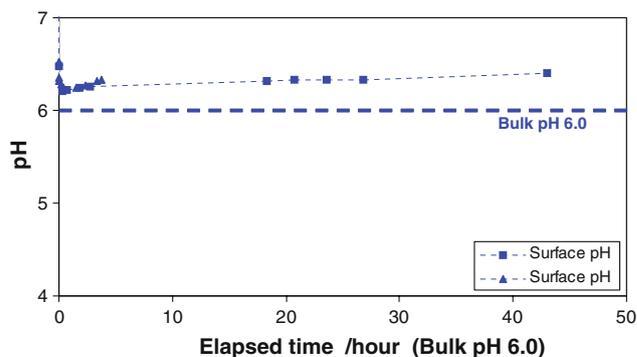

Fig. 6 Surface pH measurements during mild steel mesh corrosion in a CO_2 purged solution at bulk pH 6.0, $T = 25$ °C, $p_{total} = 1$ bar, $p_{CO_2} = 0.97$ bar, $[NaCl] = 1$ wt%
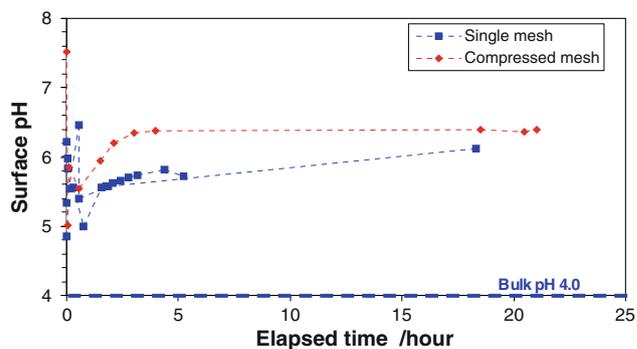

Fig. 7 The surface pH measurement comparison between a single sheet mild steel mesh and a double sheet compressed mild steel mesh at bulk pH 6.0, $T = 25$ °C, $p_{total} = 1$ bar, $p_{CO_2} = 0.97$ bar, $[NaCl] = 1$ wt%

3.2 Chemical buffer effect on surface pH

Since the pH is affected by the buffer capacity of the electrolyte, three cases are compared in Fig. 8, all at bulk pH 4.0. In a N_2 purged HCl solution, the surface pH stabilizes at 7.8, i.e., almost 4 pH units higher than the bulk pH. The surface pH increases only to 5.8 if the pH 4
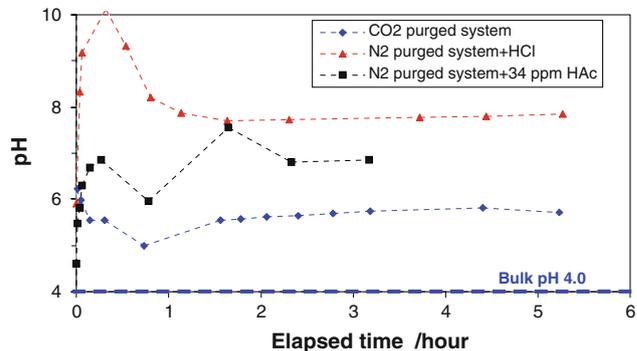

Fig. 8 Surface pH during mild steel mesh corrosion in an aqueous solution purged with CO_2 or N_2 at bulk pH 4.0, $T = 25$ °C, $p_{total} = 1$ bar, p_{CO_2} or $p_{N_2} = 0.97$ bar, $[NaCl] = 1$ wt%

solution is buffered by CO_2 where carbonic acid provides an extra source of H^+ (see reaction 6) and contributes to a lower surface pH than observed for a N_2 saturated HCl electrolyte. For an N_2 purged HAc system, the surface pH stabilizes at about 7. The degree of deviation of surface pH from the bulk value increases with decreasing buffer capacity. The highest observed surface pH values occur in systems with the least bulk solution buffering capacity.

3.3 Temperature effect on surface pH

Higher surface pH was observed at higher temperature in all the series of measurements. A comparison of surface pH at 25 and 80 °C is given in Figs. 9 (for a bare corroding mild steel mesh) and 10 (under a glass bead deposit layer, porosity 40%). The reported data correspond to steady state pH values. In all cases, slightly or significantly higher surface pH values at 80 °C were observed compared with measurements at 25 °C. In underdeposit studies with glass beads, the surface conditions can even reach alkaline at 80 °C while they remain acidic at 25 °C. This is due to the fact that the corrosion rate is higher at the higher temperature, more protons being consumed, combined with the glass beads acting as a diffusion barrier. This results in a higher observed surface pH. In addition, CO_2 dissolves less in the solution at higher temperatures and constitutes a weaker buffer solution. Water chemistry model calculation shows only half of the CO_2 dissolves at 80 °C compared with 25 °C [30]. Both mechanisms contribute to a higher surface pH at higher temperature.

3.4 Effect of deposit layer porosity on surface pH

Figures 11 and 12 show surface versus bulk pH data taken with sand and glass bead deposits, to mimic iron carbonate scale with porosity 30 and 40%, respectively, at 25 and 80
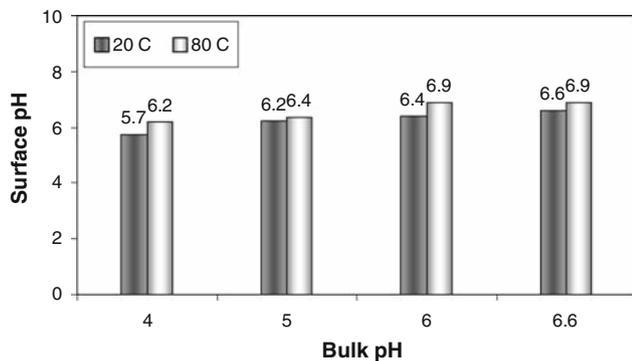
°C. When a 5-mm-thick glass bead deposit layer (particle size 50–80 μm), thick enough for diffusion affected corrosion reactions, is introduced on the mild steel mesh, the surface pH increases above pH 6, even over pH 8 in some cases at the higher studied temperature. One notices that
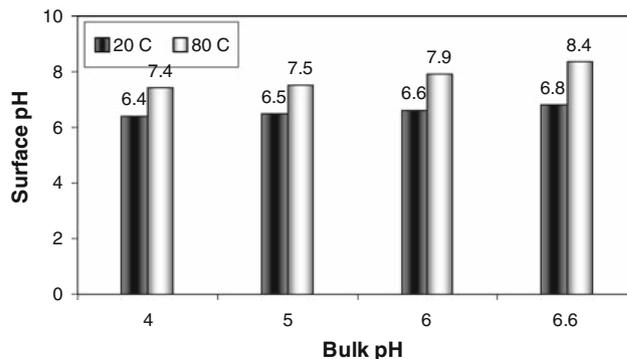

Fig. 10 Surface pH measurement during mild steel mesh corrosion under a glass bead deposit layer 5 mm in depth at different temperatures under bulk pH 4.0, 5.0, 6.0 and 6.6, $p_{CO_2} = 0.97$ bar (at 25 °C) or $p_{CO_2} = 0.53$ bar (at 80 °C) [NaCl] = 1 wt%
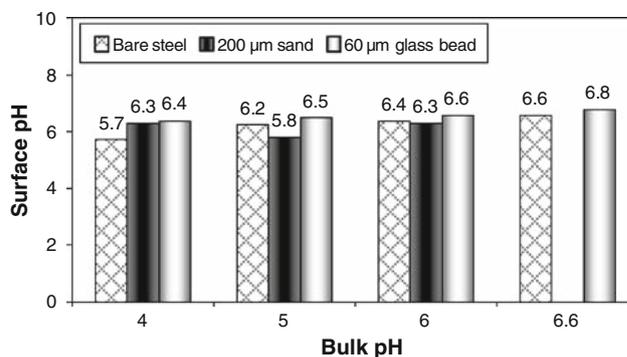

Fig. 11 Surface pH measurement for a bare mild steel mesh and those under 5 mm depth deposits, corroding at bulk pH 4.0, 5.0, 6.0 and 6.6, $T = 25$ °C, $p_{CO_2} = 1$ bar, [NaCl] = 1 wt%

Fig. 9 Surface pH comparison during a mild steel mesh corrosion, between 25 and 80 °C in a solution saturated with CO_2 under bulk pH 4.0, $p_{total} = 1$ bar, $p_{CO_2} = 0.97$ bar (at 25 °C), $p_{CO_2} = 0.53$ bar (at 80 °C), [NaCl] = 1 wt%
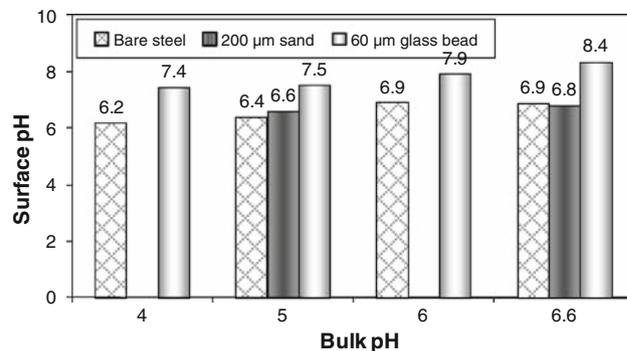

Fig. 12 Surface pH measurement for a bare mild steel mesh and those under 5 mm depth deposits, corroding at bulk pH 4.0, 5.0, 6.0 and 6.6, $T = 80$ °C, $p_{CO_2} = 0.53$ bar, [NaCl] = 1 wt%

Table 4 Surface pH measurement during mild steel mesh corroding in a CO_2 saturated solution with and without deposit layers

T (°C)	p_{CO_2} (bar)	Bulk pH of solution	Surface pH under deposit		
			Bare steel	Sand	Glass bead
25	0.97	4	5.7	6.3	6.4
		5	6.2	5. 8	6.5
		6	6.4	6.3	6.6
		6.6	6.6	NA	6.8
80	0.53	4	6.2	NA	7.44
		5	6.4	6.6	7.53
		6	6.9	NA	7.92
		6.6	6.9	6.8	8.35

the surface pH trends higher for the less porous glass bead deposit (30% porosity) compared with the more porous sand particle deposit layer (40% porosity).

3.5 Surface pH measurement at different bulk pH values

Surface pH measurement data are compiled in Table 4 for various bulk pH values and at different temperatures, all obtained in a CO_2 purged solution. For all the cases, higher surface pH was observed compared with bulk solution pH for a corroding mild steel mesh. Similarly, higher surface pH observations were made under deposit layers. Greater surface pH deviation was observed at lower bulk pH conditions. Finer glass bead deposits with a lower porosity made the surface pH deviation from the bulk larger, even in some cases reaching mildly alkaline surface conditions in an acidic bulk solution. This indicates that more alkaline local water chemistry can be achieved under the product layer during corrosion in CO_2 environments. Thus, surface conditions can develop that favour the formation of the stable passive phase magnetite (Fe_3O_4); this has been reported in the literature [4].

4 Conclusions

A mesh-based surface pH probe was developed that allows direct measurement of surface pH. Applications for the surface pH measurement were demonstrated in a mild steel corrosion system. Reproducible and stable measurements were obtained.

When compared to bulk pH, higher surface pH was obtained in all environments; this is in agreement with theoretical predictions. The largest change was obtained in a N_2 saturated HCl solution and the smallest in a CO_2 saturated solution; this is thought to be due to significant buffer capacity of the latter.

Higher surface pH deviation from the bulk was observed at higher temperature in all the series of measurements as well as at lower bulk pH conditions.

Finer glass bead deposits with a lower porosity made the surface pH deviation from the bulk pH value larger.

References

1. Han J, Yang Y, Brown B et al (2007) Corrosion/2007, paper no. 07323, Houston, TX
2. Han J, Yang Y, Brown B et al (2007) Corrosion/2008, paper no 08332, Houston, TX
3. Han J, Young D, Nešić S et al (2008) ICC/2008, paper no. 2511
4. Han J, Young D, Colijn H et al (2009) Ind Eng Chem Res 48(13):6296
5. Nordsveen M, Nešić S, Nyborg R et al (2003) Corrosion 59(5):443
6. Nešić S, Nyborg R, Stangeland A (2003) Corrosion 59(6):489
7. Nešić S, Lee K-LJ (2003) Corrosion 59(7):616
8. Dexter SC, Lin SH (1992) Corrosion 48(1):50
9. Yoshinobu T, Iwasaki H, Nakao M et al (1998) Jpn J Appl Phys Part 2 37(3B):L353
10. Yoshinobu T, Harada T, Iwasaki H (2000) Jpn J Appl Phys Part 2 39(4A):L318
11. King F, Litke CD, Tang Y (1995) J Electroanal Chem 384:105
12. Dražić DM, Djordjević S, Vojnović M (1969) 20th CITCE meeting, Strasburg
13. Lewandowski Z, Lee WC, Charazklis WG et al (1989) Corrosion 45(2):92
14. Wei C, Bard AJ, Nagy G et al (1995) Anal Chem 67:1346
15. Park J, Paik C-H, Alkire HC (1996) J Electrochem Soc 143(8):L174
16. Klusmann E, Schultze JW (1997) Electrochim Acta 42:3123
17. Honda T, Murase K, Hirato T et al (1998) J Appl Electrochem 28:617
18. Tada E, Sugawara K, Kanekol H (2004) Electrochim Acta 49:1019
19. Choi Y-S, Shim J-J, Kim J-G (2005) Corrosion 61(5):490
20. Romankiw LT (1970) IBM Tech Discl Bull 13(1):69
21. Romankiw LT (1987) Proceedings of the symposium on electrodeposition technology, theory and practice, p 301
22. Deligianni H, Romankiw LT (1993) IBM J Res Develop 37(2):85
23. Ji J, Cooper WC, Dreisinger DB et al (1995) J Appl Electrochem 25:642
24. Deslouis C, Frateur I, Maurin G et al (1997) J Appl Electrochem 27:482
25. Diaz SL, Mattos OR, Barcia OE, Fabri Miranda J et al (2002) Electrochim Acta 47:4091

26. Ordine AP, Diaz SL, Margarit ICP et al (2006) Electrochim Acta 51:1480
27. Nobial M, Devos O, Mattos OR et al (2007) J Electroanal Chem 600:87
28. Nešić S, Postlethwaite J, Olsen S (1996) Corrosion 54(4):280
29. George K, Nešić S (2007) Corrosion 63(2):178
30. Crolet JL, Bonis MR (1983) Corrosion 39(2):39